HHS Public Access

Author manuscript

J Neuroendocrinol. Author manuscript; available in PMC 2024 September 03.

Published in final edited form as:

J Neuroendocrinol. 2022 April ; 34(4): e13103. doi:10.1111/jne.13103.

PLXNB1 mutations in the etiology of idiopathic hypogonadotropic hypogonadism

Bradley A. Welch[1], **Hyun-ju Cho**[2], **Seyit Ahmet Ucakturk**[3], **Stephen Matthew Farmer**[2], **Semra Cetinkaya**[4], **Ayhan Abaci**[5], **Gamze Akkus**[6], **Enver Simsek**[7], **Leman Damla Kotan**[8], **Ihsan Turan**[8], **Fatih Gurbuz**[8], **Bilgin Yuksel**[8], **Susan Wray**[2], **A. Kemal Topaloglu**[1,9]

[1]Department of Neurobiology and Anatomical Sciences, University of Mississippi Medical Center, Jackson, MS, USA

[2]Cellular and Developmental Neurobiology Section, National Institute of Neurological Disorders and Stroke/National Institutes of Health, Bethesda, MD, USA

[3]Division of Pediatric Endocrinology, Ankara Training and Research Hospital, Ankara, Turkey

[4]Division of Pediatric Endocrinology, Dr. Sami Ulus Obstetrics and Gynecology, Pediatric Health and Disease Training and Research Hospital, University of Health Sciences, Ankara, Turkey

[5]Division of Pediatric Endocrinology, Faculty of Medicine, Dokuz Eylul University, Izmir, Turkey

[6]Division of Endocrinology, Faculty of Medicine, Cukurova University, Adana, Turkey

[7]Division of Pediatric Endocrinology, Faculty of Medicine, Eskisehir Osman Gazi University, Eskisehir, Turkey

[8]Division of Pediatric Endocrinology, Faculty of Medicine, Cukurova University, Adana, Turkey

[9]Division of Pediatric Endocrinology, Department of Pediatrics, University of Mississippi Medical Center, Jackson, MS, USA

Abstract

Correspondence: Susan Wray, Cellular and Developmental Neurobiology Section, National Institute of Neurological Disorders and Stroke/National Institutes of Health, Bethesda, MD 20892-3703, USA. wrays@ninds.nih.gov, A. Kemal Topaloglu, Department of Neurobiology and Anatomical Sciences, University of Mississippi Medical Center, Jackson, Mississippi, USA. ktopaloglu@umc.edu.
Bradley A. Welch and Hyun-ju Cho contributed equally to this work.
Susan Wray and A. Kemal Topaloglu contributed equally to this work.

AUTHOR CONTRIBUTIONS

Bradley A. Welch: Investigation, Supervision; **Hyun-ju Cho:** Methodology, Software; **Seyit Ahmet Ucakturk:** Resources; **Stephen Matthew Farmer:** Investigation, Methodology; **Semra Cetinkaya:** Resources; **Ayhan Abaci:** Resources; **Gamze Akkus:** Resources; **Enver Simsek:** Resources; **Leman Damla Kotan:** Formal analysis, Investigation, Writing – review & editing; **Ihsan Turan:** Investigation, Resources; **Fatih Gurbuz:** Resources; **Bilgin Yuksel:** Resources, Supervision; **Susan Wray:** Supervision, Writing – original draft; **A. Kemal Topaloglu:** Conceptualization, Data curation, Formal analysis, Funding acquisition, Investigation, Methodology, Project administration, Resources, Supervision, Writing – original draft, Writing – review & editing.

CONFLICT OF INTERESTS

The authors declare that they have no conflicts of interest.

PEER REVIEW

The peer review history for this article is available at https://publons.com/publon/10.1111/jne.13103.

SUPPORTING INFORMATION

Additional supporting information may be found in the online version of the article at the publisher's website.

Idiopathic hypogonadotropic hypogonadism (IHH) comprises a group of rare genetic disorders characterized by pubertal failure caused by gonadotropin-releasing hormone (GnRH) deficiency. Genetic factors involved in semaphorin/plexin signaling have been identified in patients with IHH. PlexinB1, a member of the plexin family receptors, serves as the receptor for semaphorin 4D (Sema4D). In mice, perturbations in Sema4D/PlexinB1 signaling leads to improper GnRH development, highlighting the importance of investigating PlexinB1 mutations in IHH families. In total, 336 IHH patients (normosmic IHH, $n = 293$ and Kallmann syndrome, $n = 43$) from 290 independent families were included in the present study. Six *PLXNB1* rare sequence variants (p.N361S, p.V608A, p.R636C, p.V672A, p.R1031H, and p.C1318R) are described in eight normosmic IHH patients from seven independent families. These variants were examined using bioinformatic modeling and compared to mutants reported in *PLXNA1*. Based on these analyses, the variant p.R1031H was assayed for alterations in cell morphology, PlexinB1 expression, and migration using a GnRH cell line and Boyden chambers. Experiments showed reduced membrane expression and impaired migration in cells expressing this variant compared to the wild-type. Our results provide clinical, genetic, molecular/cellular, and modeling evidence to implicate variants in *PLXNB1* in the etiology of IHH.

Keywords

hypogonadotropic hypogonadism; PLXNB1; puberty

1 | INTRODUC TION

Idiopathic hypogonadotropic hypogonadism (IHH) comprises a group of rare genetic disorders characterized by complete or partial pubertal failure caused by gonadotropin-releasing hormone (GnRH) deficiency. According to olfactory function, IHH is divided into two major clinical forms: normal sense of smell (normosmic IHH, nIHH) and inability to smell, anosmia, known as Kallmann syndrome (KS). However, this distinction is often unclear, reflecting the spectrum of pathophysiological mechanisms. Almost 60 genes have been reported to be associated with IHH. Yet these genes account for approximately 50% of all cases, suggesting that other associated genes remain to be discovered.[1,2] To date, the genes implicated in IHH are involved in GnRH neuron ontogenesis, GnRH neuron migration, GnRH secretion or gonadotrope function. GnRH-secreting neurons are unique in that they are born outside the central nervous system in the nasal placode and migrate to the hypothalamus along the vomeronasal and terminal nerves during embryonic development.[3] This journey is evolutionarily highly conserved and follows a similar pattern in all mammals,[3] including humans.[4,5] Orchestration of numerous factors/cues participates in this process to ensure GnRH cells reach the forebrain because aberrant development of this neuroendocrine system results in IHH. Understanding the pathogenesis leading to IHH in humans uncovers genetic pathways critical to the development or function of GnRH neurons and potential therapies.

Semaphorins, a large and diverse family of secreted and membrane-associated proteins, act as neuronal guidance cues during embryogenesis,[6] including targeting of GnRH neurons and olfactory/vomeronasal projections.[7] PlexinB1, a member of the Plexin

family receptors,[8,9] interacts with semaphorin 4D (Sema4D). Signaling through this ligand–receptor coupling plays a role in dendrite remodeling,[10] axonal guidance,[11] bone development,[12] organogenesis,[13] angiogenesis,[14] and cell motility.[15,16] During cell migration, PlexinB1 reorganizes actin cytoskeleton by activating Rho family GTPases[17] and initiates growth cone collapse.[18] In mice, perturbations in PlexinB1/Sema4D signaling lead to improper GnRH development,[19,20] yet no human mutations in this pathway related to GnRH development have been documented so far.

To initiate signaling, monomers of PlexinB1 receptor are brought together to form dimers by Sema4D.[21] PlexinB1 contains three cysteine-rich PSI (plexin, semaphorin, integrin) domains and six IPT domains (Ig domain shared by plexins and transcription factors). Once activated (dimerized by ligand), the PlexinB1 catalytic domain assembly can (1) enable intracellular Rho GTPases to directly or indirectly bind to multiple proteins including Rnds, Racs, Rhos, and Ras[22]; (2) regulate GTPase activity through an intrinsic GTPase-activating protein (GAP) domain, as well as a direct interaction with Rho guanine nucleotide exchange factor proteins (Rho GEFs), PDZ-Rho GEF and LARG, through its PDZ binding motif[23]; or (3) couple signal transduction through other kinase receptors such as ErbB-2 and Met.[24] Thus, PlexinB1 can signal through multiple pathways to initiate changes in actin cytoskeleton, axon guidance, invasive cell growth, and cell migration.

Another semaphorin receptor, PlexinA1, with a structure similar to that of PlexinB1, has been implicated in the migration of GnRH neurons and the etiology of KS[25,26] as well as nIHH,[27] although individual analysis of these mutations was not confirmed in bioassays. In the present study, six *PLXNB1* rare sequence variants are described in eight IHH patients. These variants were located in different regions of the extracellular (ecto) domain of PlexinB1 (p.N361S, p.V608A, p.R636C, p.V672A, p.R1031H, and p.C1318R). These variants were examined using bioinformatic modeling and compared to mutants reported in PlexinA1. Based on these analyses, one variant, p.R1031H, was assayed and shown to induce alterations in cell morphology, PlexinB1 expression, and migration using a GnRH cell line and Boyden chambers.

2 | MATERIALS AND METHODS

2.1 | Patients

In total, 336 IHH patients (nIHH, $n = 293$ and KS, $n = 43$) from 290 independent families recruited in Turkey were included in the present study. IHH patients had absent pubertal development by age 13 years and 14 years in girls and boys, respectively, and low or inappropriately normal basal gonadotropin levels in the face of low sex steroid levels. In most cases, a GnRH stimulation tests were carried out to aid in diagnosis. The levels of olfactory function were determined based on self-reporting and physical examination by administering a culturally appropriate 10-item (mint, lemon, soap, etc.) smell test. These patients were clinically followed every 4–6 months by referring pediatric endocrinologists at least until young adulthood because the diagnosis of IHH often requires long follow-up periods. All individuals and/or their legal guardians provided written informed consent, and the study was approved by the Ethics Committee of the Cukurova University Faculty of

Medicine and by the institutional review board of the University of Mississippi Medical Center.

2.2 | DNA sequencing and rare variant analyses

The genomic DNA samples for exome sequencing were prepared as an Illumina sequencing library and, in the second step, the sequencing libraries were enriched for the desired target using the Illumina Exome Enrichment protocol. The captured libraries were sequenced using an Illumina HiSeq 2000 Sequencer. The reads were mapped against UCSC (https://genome.ucsc.edu/cgi-bin/hgGateway) hg19. Exome data variant filtering was performed using wANNOVAR[28] to annotate functional consequences of genetic variation and to pinpoint a specific subset of variants most likely to be causal for IHH. The variants in exome sequencing data were filtered against population polymorphism databases such as Gnomad (https://gnomad.broadinstitute.org) or the Greater Middle East Variome (GME) (http://igm.ucsd.edu/gme/data-browser.php). Additionally, ethnic-specific harmless polymorphisms were filtered out by comparing against in-house data from 132 Turkish adult individuals who were known not to have a history of puberty/infertility problems. The presence and segregation of significant variants within pedigrees were verified by Sanger sequencing on an PRISM 3130 auto sequencer (Applied Biosystems).

2.3 | Molecular modeling

Human PlexinB1 ectodomain was modeled with I-TASSER (PlexinB1$^{ecto(I-TASSER)}$) using amino acids 1–1490 (UniProtKB: O43157).[29,30] PlexinB1$^{ecto(I-TASSER)}$-Sema4D^{ecto} was artificially constructed by superimposing PlexinB1$^{ecto(I-TASSER)}$ onto co-crystallized PlexinB1$^{ecto(fragment)}$ (amino acids 26–533) bound to Sema4D^{ecto} (Protein Data Bank: 3OL2). The I-TASSER-predicted region (amino acids 26–533) was morphed to the co-crystal fragment (amino acids 26–533) in PyMOL (Schrödinger, LLC) to preserve binding groves and fused to full-length PlexinB1$^{ecto(I-TASSER)}$ using UCSF Chimera (https://www.cgl.ucsf.edu/chimera). TM-score (http://zhanglab.ccmb.med.umich.edu/TM-score) was used to validate whether the morphed region of PlexinB1$^{ecto(I-TASSER)}$ was in the same fold as the PlexinB1$^{ecto(fragment)}$ crystal (TM-score = 1.00; RMSD = 0.00).[31,32] The signaling complex was then energy minimized using YASARA.[33] ResProx (resolution = 1.738 Å) and MolProbity (score = 1.99; 76th percentile) were used to validate the quality of the energy-minimized complex.[31,34] MutaBind2, mCSM-PPI2, and SAAMBE were used to predict the effects on protein–protein binding free energy.[35–37] DynaMut and PremPS were used to predict the effects on protein folding/unfolding free energy.[38,39]

2.4 | Cell culture

The immortalized GnRH cell line, Gn11,[40] was kindly provided by Dr T. John Wu (Uniformed Services University of the Health Sciences, Bethesda, MD, USA).[41] Cells were grown in monolayer (37°C, 5% CO_2) in Dulbecco's modified Eagle's medium (Phenol Red Free, catalog. no. 17-205-CV; Mediatech) supplemented with 25 mM glucose (ICN Biomedicals, Inc.), 5 mM L-glutamine (A2916801; Gibco), and 10% fetal bovine serum (FBS) (Life Technologies, Inc.) without antibiotics. Cells were given fresh medium at 2-day intervals and subcultured from 80% confluent to 20% by trypsinization.

2.5 | Generation of lentiviral vectors

The coding sequence for human *PLXNB1* (NM_001130082.2, catalog. no. 70469; Addgene) was subcloned into the pLL3.7 Lentiviral vector together with a N-terminal 3X FLAG tag sequence. For the mutant plasmid, two partial *PLXNB1* CDS fragments flanking the point mutation were amplified by overlapping primers bearing the mutation. The fragments (3X FLAG tag and two fragments of *PLXNB1*) were assembled into pLL3.7 plasmid using the In-Fusion cloning system (catalog. no. 638909; Takara Bio). Sequencing was performed to confirm the correct modifications were made on each plasmid. The primers for cloning are shown in the Supporting information (Table S1). Wild and mutant lentiviruses were generated by the NINDS Viral Production Core Facility (Bethesda, MD, USA). Lenti-CMV-GFP was used as the control vector.

2.6 | Transduction of Gn11 cells

Gn11 cells were plated in 24-well plates and transduced with control, wild, and mutant *PLXNB1* lentiviral vectors at a multiplicity of infection of 8 and 16 in the presence of 8 μg mL^{-1} polybrene (Sigma-Aldrich). Transduction efficiency was over 95% as determined by green fluorescent protein expression in cells transduced by control vector (data not shown). Cells were subcultured and maintained in phenol red free Dulbecco's modified Eagle's medium supplemented with 10% FBS until validated and analyzed for migration assays. Eleven days after transduction, cells were harvested for RNA prep and subsequently validated for *PLXNB1* expression by a real-time polymerase chain reaction (RT-PCR) (Figure S1).

2.7 | PlexinB1 immunostaining on Gn11 cells

Control or *PLXNB1* transduced Gn11 cells were plated and grown on glass coverslips until approximately 60% confluency (two coverslips/group/two different platings). Cells were then fixed (4% formaldehyde/1 × phosphate-buffered saline [PBS]), treated with or without 0.2% Triton X-100/10% NHS/1 × PBS for 10 min (membrane permeabilization), washed three times with 1 × PBS and blocked in 10% NHS/1X PBS for 1 h. Rabbit anti-*PLXNB1* antibody (dilution 1:500 in 1% BSA/1 × PBS, 4°C, overnight; catalog. no. 23795-1-AP; Proteintech) and Alexa Fluor 555 conjugated donkey anti-rabbit (dilution 1:1000 in 1 × PBS, room temperature, 1 h, catalog. no. A31572; Thermo Fisher Scientific) were used for standard immunofluorescence staining. Nuclei were stained with 4′,6-diamidino-2-phenylindole (DAPI) and cells coversliped using Fluoro-Gel Mounting Medium (Electron Microscopy Sciences). Three images per group per coverslip were captured using an Eclipse E800 upright microscope (Nikon) at 40×. Images were analyzed to obtain the cell area and integrated density of PlexinB1 staining using Fiji/ImageJ (NIH).

2.8 | Boyden chamber assays

Boyden chambers (8.0 μm Transparent PET Membrane, catalog. no. 353097, Falcon; Corning Inc.) were used for migration assays.[19] Cell lines: Gn11 no infection, Gn11 mock (Lenti-CMV-GFP), and Gn11 transduced with Lenti-CMV-3XFLAG-hPLXNB1 (WT and p.R1031H) were used within seven passages for experiments. Forty-eight hours prior to assaying, subconfluent cells were fed reduced serum media (5% FBS) in serum-free media

(SFM) overnight, and then 1% FBS in SFM overnight to reduce cell division. Boyden chambers were placed in 24-well plates, coated with poly-D-lysine (Sigma-Aldrich; room temperature, 10 min, washed twice with distilled H_2O 24 h prior to chemotactic assays). Cells (3.5×10^4 cells/200 μl SFM) were added to the top chambers, and 700 μl of SFM alone or SFM supplemented with drugs was added to the bottom chambers (Recombinant human semaphorin 4D, rhSema4D 0.625, 1.25, 2.5, 5.0 or 7.5 nM, catalog. no. 11825-H08H; SinoBiological, or Recombinant mouse hepatocyte growth factor [HGF], 0.5 nM, catalog. no. 2207-HG-025/CF; R&D Systems). HGF served as a positive control for all assays because it directly induces GnRH cell migration via activation of its receptor Met,[42] and indirectly via coupling signaling through PlexinB1.[19] Plates were kept in a humidified incubator (37°C with 5% CO_2) for 6 h.

After incubation, the chambers were fixed (4% formalin, room temperature, 30 min), washed and blocked (10% normal horse serum/0.3% Triton X-100, room temperature, 30 min). Membranes were carefully cut out and the top chamber cells were physically removed with a cotton swab soaked in 1 × PBS. Membranes containing cells that had migrated through the membrane were then incubated with guinea pig anti-DcX primary (Chemicon; dilution 1:3500 in 1% bovine serum albumin [BSA]/0.1% NaN_3/PBS, 4°C for 48–72 h), washed (1 × PBS), and then incubated in Alexa Fluor 488 conjugated donkey anti-guinea pig secondary (Invitrogen; dilution 1:1000 in 0.1% Triton X-100/PBS, room temperature, 2 h). Chambers were then treated with BSA (1% BSA/0.1% NaN_3/PBS, room temperature, 30 min) to prevent non-specific background from methanolic phallotoxin solution, washed (1 × PBS), incubated with Alexa Fluor 555 Phalloidin (Thermo Fisher; dilution 1:80 in PBS, room temperature, 45 min), washed, and incubated with DAPI (dilution 1:1000 in PBS, room temperature, 10 min). Membranes were mounted with the bottom side up and cover-slipped with Fluoro-Gel Mounting Medium (Electron Microscopy Sciences) and digitized after drying.

2.9 | Image analysis

For each chamber, cells that migrated were imaged (four random 10× fields) using an Eclipse E800 upright microscope (Nikon). DcX+/Phalloidin+/Dapi+ cells were counted using Fiji/ImageJ software for all four fields and averaged to get cells/field for each chamber (i.e., total cells divided by four fields). For each independent experiment, treatments were run in duplicate (i.e., two chambers per treatment per experiment). The mean cells/field for each duplicate per independent experiment was used for analysis (n = independent experiments). For testing the effect of varying Sema4D concentrations and differences between no infection and mock infection, migratory cell numbers were normalized using SFM values between experimental trials. Unless otherwise specified, data were analyzed using a one-way ANOVA, followed by Fisher's post-hoc least significant difference.

3 | RESULTS

We identified heterozygous missense variants in *PLXNB1* (HGNC: 9103, NM_001130082.2) in eight patients from seven unrelated families. Figure 1 shows the family pedigrees with variant segregations. Clinical and molecular genetic characteristics of

the patients and their alterations are shown in Tables 1 and 2, respectively. These six variants were either not seen or were extremely rare with a minor allele frequency < .0001 in the largest reference population database, gnomAD. Similarly, these variants were not reported in a much smaller but regional database, the Greater Middle East Variome (GME).[43] Sanger sequencing confirmed the presence of these variants. No variant was seen in ClinVar (https://www.ncbi.nlm.nih.gov/clinvar). These variants were all classified as variants of uncertain significance (VUS) by ACMG/AMP classification.[44] Detailed information regarding these variants is provided in Table 2.

Table 1 depicts the clinical and laboratory characteristics of individuals with PLXNB1 mutations at initial presentations and after prolonged follow-up periods. All patients presented with delayed pubertal development. To confirm the etiology of delayed puberty, specifically discriminating IHH from constitutional delay in growth and puberty (CDGP), often requires periodical physical and laboratory evaluations. Notably, patient A I-1, the father of patient AII-2, who, by history, presented with pubertal delay, started normal pubertal development at age 17 years. His son (AII-2) has also shown spontaneous pubertal development around 18 years of age, attaining bilateral testicular volumes of 20 ml with adult level hormonal values at age 20 (Table 1). These observations are consistent with CDGP. This father and son duo also carries a CCDC141 variant. Recently, mutations in CCDC141 were reported as a frequent finding in patients with CDGP.[45] Therefore, the CCDC141 variant in Family A appears to account for delayed puberty. However, patient B II-1, who has the final diagnosis of IHH, possesses the same PLXB1 variant without any CCDC141 or any other IHH gene mutations. Collectively, these results indicate an oligogenecity in Family A, also indicating mutations in more than one IHH gene contributed to the phenotype observed, which is seen in 10%–20% of all IHH cases.[46] In Family C, the patient had a history of cryptorchidism as an infant, suggesting that severe congenital hypogonadism as the fetal testicular descent is androgen-dependent. Nevertheless, he presented at age 21 years again with partial hypogonadotropic hypogonadism based on early to mid-pubertal testicular sizes (8 mL bilaterally) with subnormal gonadotropin and testosterone levels for age (Table 1). On follow-up with testosterone replacement, his testicles remained mid-pubertal at age 28 years. This clinical picture of severe congenital HH followed by clinical recovery as a young adult, albeit partial in this case, has been observed previously, particularly in those who have TAC3/TACR3 mutations.[47] All of the remaining five patients have shown complete IHH with no evidence of spontaneous pubertal development well beyond age 18 years (Table 1). In Family E and Family G, patients inherited PLXNB1 variants from their unaffected mothers. In Family F, the mutation appears to be de novo (Figure 1). In Families B, C, and E, the inheritance (autosomal dominant vs. de novo) is unclear as a result of insufficiency in parental DNA availability. In Family A and F, there were additional variants in IHH-associated genes. Because, in Family A, only the son has the DMXL2 variant and not the father with the same phenotype, it is unclear whether the DMXL2 variant contributed to the IHH phenotype in the son (Figure 1). In Family F, we consider that the de novo mutation may account for the phenotype. Again, it is unclear whether the RAB3GAP1 variant from the unaffected mother influenced this patient's phenotype. Overall, the inheritance pattern of IHH as a result of the PLXNB1 variants appear to best fit with an autosomal dominant inheritance with variable expressivity,

which was repeatedly observed in recent IHH gene discoveries.[48,49] Oligogenic etiology[46] and clinical recovery,[50] amongst others, are well recognized in this condition as explaining these complex pedigrees.

A schematic and model of semaphorin/plexinB1 dimers are shown in Figure 2A. semaphorin/plexinB1 dimers were modeled using a co-crystal fragment dimer (Protein Data Bank: 3OL2) (Figure 2A, right). The six *PLXNB1* variations (p.N361S p.V608A, p.R636C, p.V672A, p.R1031H, and p.C1318R) (Figure 2A, left) were examined using in silico mutagenesis. Multiple analyses consistently predicted that p.V608A (located in the IPT1 domain), p.V672A (located in the Mucin domain) and p.R1031H (located in the PSI3 domain) were deleterious to the interaction of PlexinB1 with its binding partners and to its protein folding (Figure 2B, highlighted in gray; see also Supporting information, Table S2). PlexinB1 mutants were then aligned with PlexinA1 mutants found in normosmic and anosmic IHH patients (Figure 3).[25,27] There are no variants reported in the IPT1 domain of PlexinA1 (i.e., compared to p.V608A in PlexinB1) and PlexinA1 does not have a Mucin domain. By contrast, four variants were reported in the PSI3 domain of PlexinA1 (p.R813H, p.R836H, p.R840Q, p.A854T), within the same domain as p.R1031H found in PlexinB1 (Figure 3). Based on the confluence of mutations in the PSI3 domain and the occurrence the PSI3-domain mutation p.R1031H in two independent pedigrees, the functional property of the p.R1031H variant on GnRH migration was further investigated using an immortalized GnRH cell line, Gn11,[40,51] in Boyden chamber chemotaxis assays.

3.1 | Attenuated membrane expression of PlexinB1 variant (P.R1031H) on transduced Gn11 cells

Mock (Lenti-CMV-GFP), WT and MT (p.R1031H) human *PLXNB1* (*hPLXNB1*) were introduced into Gn11 cells using recombinant Lentiviruses. Transduced Gn11 cells were validated for *hPLXNB1* overexpression via RT-PCR and sequencing (see Supporting information, Figure S1). To determine whether the variant changed expression and/or location of the plexinB1 protein, the cell area, total PlexinB1, and membrane PlexinB1 expression were compared (see Supporting information, Figure S2). None and Mock treated Gn11 cells were first compared (see Supporting information, Figure S2A). Relative mean cell areas obtained from None and Mock groups showed no effect on cell size after viral transduction ($p = .7271$). Integrated densities of PlexinB1 staining on cells with Triton X-100 permeabilization represents total PlexinB1 expression (inside and outside), whereas those on cells without permeabilization represents membrane PlexinB1 only. The relative expression of total and membrane PlexinB1 showed no significant difference between None and Mock groups for either condition ($p = .1756$ and $p = .1506$, respectively). Next, the same measurements were performed on Mock, transduced WT and transduced MT cells. Cell area was significantly reduced (by approximately 30%) in the MT group compared to both Mock and WT cells ($p < .0001$ for both comparison) (see Supporting information, Figure S2B). Total PlexinB1 expression was significantly increased by viral transduction in WT compared to mock ($p = .0253$). By contrast, the MT was not significantly different from mock, and it was also not significantly different from WT (Figure S2B). These results suggest incomplete protein synthesis or degradation of mutant caused by protein instability which is predicted from in silico analysis (see Supporting information, Table S2). Notably,

membrane localized PlexinB1 showed a significant increase in WT compared to both Mock and MT (see Supporting information, Figure S2B), although no differences between Mock and MT ($p = .1122$), consistent with the variant attenuating the amount/ability of the MT protein to associate with the plasma membrane.

3.2 | P.R1031H impairs hPLXBN1 response to PLXNB1 agonists

To determine the functional consequences of the p.R1031H mutation on PlexinB1 function, migration assays were run in which Gn11 cells were plated on the top membrane of a Boyden chamber and a chemoattractant was added beneath the chamber. Cells that migrate to the chemoattractant move through the Boyden chamber membrane, ending up on the bottom membrane surface. At the end of the experiment, non-migratory cells on the top surface are removed and the migratory cells on the bottom surface were stained with DcX (marker for migratory neurons)/Phalloidin (marker for F-actin)/DAPI (nuclei marker; see Supporting information, Figure S3A) and quantified. Initial migration experiments were performed using Gn11 cells with no infection and varying concentrations of rhSema4D (0.625–7.5 nM). These experiments established that exposure to 1.25 and 2.5 nM rhSema4D increased the number of triple labeled Gn11 cells that had migrated compared to SFM control ($p = .0111$, $p = .0028$, respectively) (see Supporting information, Figure S3B,C). Next, experiments were performed comparing the migration of Gn11 cells with no infection to Gn11 mock infected (Lenti-CMV-GFP) across treatments. Independent of treatment, no differences in response between these two cell groups was detected (two-way ANOVA; treatment $p = .3918$), indicating no change in cell viability or ability to migrate after Lenti-CMV-GFP mock infection (Figure S3D,E).

A series of experiments was then performed using 2.5 nM rhSema4D as the attractant for Gn11 cells that were infected by mock (Lenti-CMV-GFP) or one of two Lenti-CMV-3XFLAG-hPLXNB1 constructs (+hWT or +hR1031H) (Figure 4A,B) and cellular migration was assayed. Transduced Gn11 cells were validated for *hPLXNB1* overexpression via RT-PCR and sequencing (see Supporting information, Figure S1). When exposed to just SFM in the bottom well, Gn11 cells +hWT exhibited an overall increase in migratory cells/field for SFM compared to all other groups ($n = 3$, +hWT vs. mock, $p = .0009$; +hWT vs. +hR1031H, $p = .0022$) (Figure 4B). In agreement with our earlier experiments, when exposed to rhSema4D, cell migration increased in the mock group compared to SFM alone, showing the basal level of endogenous PlexinB1 function ($n = 3$, $p = .0073$). However, the number of migratory cells in the bottom chamber significantly increased in the +hWT group exposed to rhSema4D compared to mock exposed to rhSema4D ($n = 3$, $p = .0010$) (Figure 4B). By contrast, the number of migratory cells in the bottom chamber significantly decreased in the +hR1031H group +rhSema4D compared to mock +rhSema4D ($p = .0009$). Notably, the migration of cells in +hR1031H + rhSema4D was similar to that of its SFM group, as well as the mock SFM group. Migration in all cell groups exposed to HGF was similar to that detected in the corresponding cell groups exposed to rhSemaD (Figure 4B). In addition, rhSema4D and HGF increased migration in mock control cells ($n = 3$, rhSema4D, $p = .0073$; $n = 3$, HGF, $< p = .0001$) and cells expressing hWT hPLXNB1 ($n = 3$, rhSema4D, $p = .0079$; $n = 3$, HGF, $< p = .0001$). Notably, +hR1031H showed no response to rhSema4D or HGF, remaining at levels similar to the SFM mock group. These data indicate that this

mutation alters direct (via Sema4D) and indirect (via HGF/Met) PlexinB1 pathways. At the protein level, p.R1031H not only destabilized PlexinB1 folding and binding to Sema4D (see Supporting information, Table S2), but also diminished intrachain bonds (Figure 4C,D), which may affect how the protein is held together, its dimerization, or its putative flexibility to activate upon ligand or co-receptor binding.

4 | DISCUSSION

The present study identifies PLXNB1 signaling as a requirement for timely pubertal onset in humans. We present both clinical and molecular genetic data from eight patients from seven independent families who presented with pubertal failure. The PLXNB1 variants identified were characterized via in silico analysis and compared to human variants published for PLXNA1, and one variant was selected for functional analysis. Transduction of a GnRH cell line with lentiviral vectors carrying the *PLXNB1* variant significantly reduced neuronal migration. These data are consistent with PLXNB1 signaling comprising an important cue in vivo that ensures GnRH neurons migrate into the brain for subsequent activation of reproductive function.

Semaphorins constitute one of the largest protein families of phylogenetically conserved guidance cues, and their primary transducing receptors belong to the plexin family.[52] Our studies on semaphorin signaling mutations in the etiology of IHH,[27,53] including the present one, reveal that 25 of the 290 probands (8.6%) in our IHH cohort harbor mutations in semaphorins and/or their receptors. This indicates that genes in the semaphorin signaling pathway, along with the FGF group genes[54] and CHD7,[1,2,55] are the most frequently mutated gees in congenital GnRH deficiency.

Genetic factors involved in semaphorin/plexin signaling identified from patients with IHH, include *SEMA3A*,[56–58] *SEMA3E*,[59] *SEMA3F*,[53] *SEMA3G*,[60] *SEMA4D*,[61] *SEMA7A*,[57] *PLXNA1*,[25,27] and *PLXNA3*.[53] As for PLXNB1, a previous screening study in 138 adult males for IHH genes reported nine *PLXNB1* variants, which were not specified by cDNA or amino acid change.[61] In one study, *PLXNB1* variants were concomitantly seen with truncating mutations in ANOS1 or CHD7[38] In another study, a PLXNB1 variant was seen in addition to GNRHR and AXL variants in one patient.[62] Overall, it is not clear whether PLXNB1 variants added to the respective disease severity in those cases.[62,63] To the best of our knowledge, this is the first study to focus on PLXNB1 variants as a direct cause of IHH.

PLXNB1 has been considered a candidate gene for IHH based on animal studies showing reduced hypothalamic GnRH content in *Plxnb1*$^{-/-}$ mice[19] and Sema4d$^{-/-}$ mice.[64] In the *Plxnb1*$^{-/-}$ mice, a reduction in the number of GnRH neurons in the brain was reported at embryonic day 14.5. However, the total GnRH cell number remained constant at embryonic day 14.5 and postnatal day 3 between knockout and wild-type, with more cells located at the level of the nasal forebrain junction/olfactory bulbs in knockouts. Correlated with the reduced GnRH cell number in the brain of adult *Plxnb1*$^{-/-}$ mice, the number of GnRH immunoreactive fibers in the median eminence, where these cells release GnRH hormone into the portal system, was also significantly reduced.[19] These data indicate that the GnRH cells were able to migrate to the nasal forebrain junction and suggest that entrance into

the forebrain was perturbed, allowing fewer GnRH cells into the forebrain proper. Notably, examination of the olfactory/vomeronasal axons, on which the GnRH neurons migrate to the nasal forebrain junction, uncovered no abnormalities in the *Plxnb1*$^{-/-}$ mice.[19] In addition, using another *Plxnb1* knockout model, Deng et al.[64] reported that the development of the olfactory bulb in the knockout was similar to wild-type, noting that the projection of the olfactory nerves to the olfactory bulb was normal. As such, the two PLXNB1 knockout studies[19,64] suggest that the loss of PLXNB1 does not perturb the developing olfactory system, predicting a normosmic phenotype with PLXNB1 variants. Indeed, all eight patients in the present study have a normal sense of smell (normosmic). To date, most semaphorin signaling gene variant discoveries (except for SEMA3F and PLXNA3), were carried out solely in KS patient co-horts.[25,56,58] This may have obscured the olfactory phenotypic spectrum associated with semaphorins. Indeed, the seminal publication on PLXNA1was from an all anosmic (KS) cohort.[25] Yet a previous screening study of PLXNA1 mutant cases, conducted in the same cohort as that used in the present study, revealed nine cases, among which only one-third had hyposmia/anosmia.[27]

We used Boyden chamber assays to determine whether mutant PLEXNB1 can cause impairment in GnRH neuron migration. In Boyden chamber assays, additional expression of human PlexinB1 (+hWT) in Gn11 cells increased cell migration compared to the mock group, indicating that it augmented cell migration in the presence of endogenous PlexinB1 levels. These data indicate that expression of +hWT increases the cell's basal level of migratory activity even in the absence of ligand (SFM). The increase detected with hWT hPLXNB1 could be a result of non-soluble/membrane bound Sema4D on neighboring cells directly interacting with +hWT,[65,66] endogenous autocrine/paracrine-released Sema4D propagating signals,[11] or reciprocal interactions with ErbB-2 and Met.[24] In the presence of rhSema4D or HGF, mutant human PlexinB1 reduced migration compared to either the hWT or the mock group. These results indicate that introduced human mutant PlexinB1 inhibited the function of the endogenous PlexinB1 in Gn11 cells. Possible scenarios of this inhibition could be (1) most of the ligands are occupied by overexpressed mutant PlexinB1 (non-functional) and not available for endogenous PlexinB1 and/or (2) mutant PlexinB1 forms dimer with endogenous PlexinB1 and inhibits their function. Arguing against the former explanation is the fact that p.R1031H, being in the extracellular domain, was predicted to destabilize PlexinB1-Sema4D direct interactions. In addition, similar cell migration was detected in mock and mutant PlexinB1 (+hR1031H) cells in the absence of ligands (SFM), consistent with a ligand-initiated perturbation in the mutant cells. As such, the data are consistent with the mutant PlexinB1 forming dimers with the endogenous PlexinB1 and inhibiting their function. In the presence of ligands, the loss of responsiveness of immortalized GnRH cells transduced with the mutant PlexinB1, as well as the predicted deleterious structural effects induced by p.R1031H, corroborate that this mutation underlies the phenotype found in the IHH patients. Considering that this mutation was found as heterozygous in the IHH patients highlights a dominant-negative effect of the mutation in the pathogenic mechanism of *PLXNB1*.

In summary, we provide clinical, genetic, molecular/cellular, and modeling evidence to implicate variants in *PLXNB1* signaling in the etiology of IHH. These studies add to the growing number of semaphorin signaling molecules in GnRH ontogeny, and thus

mutations in the pathogenesis of pubertal failure. Semaphorin signaling genes should be in the diagnostic panels for normosmic as well as anosmic HH cases because they account for one of the largest group of genes in the etiology of IHH.

Supplementary Material

Refer to Web version on PubMed Central for supplementary material.

ACKNOWLEDGMENTS

The present study was supported by a start-up grant (DN00305) by UMMC to AKT. The study was also supported by the Cukurova University Scientific Research Project number 11364. The work was partly supported by the Intramural Research Program of the National Institutes of Health, National Institute of Neurological Disorders and Stroke (ZIA NS002824) to SW. No funding for the remaining authors was received for the present study.

Funding information

UMMC, Grant/Award Number: DN00305; Cukurova University, Grant/Award Number: TSA11364; Foundation for the National Institutes of Health, Grant/Award Number: ZIA NS002824

DATA AVAILABILITY

The data that support the findings of this study are available from the corresponding author upon reasonable request.

REFERENCES

1. Howard SR, Dunkel L. Delayed puberty-phenotypic diversity, molecular genetic mechanisms, and recent discoveries. Endocr Rev. 2019;40(5):1285–1317. [PubMed: 31220230]
2. Witchel SF, Plant TM. Neurobiology of puberty and its disorders. Handb Clin Neurol. 2021;181:463–496. [PubMed: 34238478]
3. Wray S, Grant P, Gainer H. Evidence that cells expressing luteinizing hormone-releasing hormone mRNA in the mouse are derived from progenitor cells in the olfactory placode. Proc Natl Acad Sci USA. 1989;86(20):8132–8136. [PubMed: 2682637]
4. Casoni F, Malone SA, Belle M, et al. Development of the neurons controlling fertility in humans: new insights from 3D imaging and transparent fetal brains. Development. 2016;143(21):3969–3981. [PubMed: 27803058]
5. Schwanzel-Fukuda M, Pfaff DW. Origin of luteinizing hormone-releasing hormone neurons. Nature. 1989;338(6211):161–164. [PubMed: 2645530]
6. Pasterkamp RJ. Getting neural circuits into shape with semaphorins. Nat Rev Neurosci. 2012;13(9):605–618. [PubMed: 22895477]
7. Giacobini P Shaping the reproductive system: role of semaphorins in gonadotropin-releasing hormone development and function. Neuroendocrinology. 2015;102(3):200–215. [PubMed: 25967979]
8. Hu S, Zhu L. Semaphorins and their receptors: from axonal guidance to atherosclerosis. Front Physiol. 2018;9:1236. [PubMed: 30405423]
9. Junqueira Alves C, Yotoko K, Zou H, Friedel RH. Origin and evolution of plexins, semaphorins, and Met receptor tyrosine kinases. Sci Rep. 2019;9(1):1970. [PubMed: 30760850]
10. Tasaka G, Negishi M, Oinuma I. Semaphorin 4D/Plexin-B1-mediated M-Ras GAP activity regulates actin-based dendrite remodeling through Lamellipodin. J Neurosci. 2012;32(24):8293–8305. [PubMed: 22699910]
11. Masuda K, Furuyama T, Takahara M, Fujioka S, Kurinami H, Inagaki S. Sema4D stimulates axonal outgrowth of embryonic DRG sensory neurones. Genes Cells. 2004;9(9):821–829. [PubMed: 15330859]

12. Negishi-Koga T, Shinohara M, Komatsu N, et al. Suppression of bone formation by osteoclastic expression of semaphorin 4D. Nat Med. 2011;17(11):1473–1480. [PubMed: 22019888]
13. Korostylev A, Worzfeld T, Deng S, et al. A functional role for semaphorin 4D/plexin B1 interactions in epithelial branching morphogenesis during organogenesis. Development. 2008;135(20):3333–3343. [PubMed: 18799546]
14. Fazzari P, Penachioni J, Gianola S, et al. Plexin-B1 plays a redundant role during mouse development and in tumour angiogenesis. BMC Dev Biol. 2007;7:55. [PubMed: 17519029]
15. Basile JR, Afkhami T, Gutkind JS. Semaphorin 4D/plexin-B1 induces endothelial cell migration through the activation of PYK2, Src, and the phosphatidylinositol 3-kinase-Akt pathway. Mol Cell Biol. 2005;25(16):6889–6898. [PubMed: 16055703]
16. Zhou C, Wong OG, Masters JR, Williamson M. Effect of cancer-associated mutations in the PlexinB1 gene. Mol Cancer. 2012;11:11. [PubMed: 22404908]
17. Barberis D, Casazza A, Sordella R, et al. p190 Rho-GTPase activating protein associates with plexins and it is required for semaphorin signalling. J Cell Sci. 2005;118(Pt 20):4689–4700. [PubMed: 16188938]
18. Ito Y, Oinuma I, Katoh H, Kaibuchi K, Negishi M. Sema4D/plexin-B1 activates GSK-3beta through R-Ras GAP activity, inducing growth cone collapse. EMBO Rep. 2006;7(7):704–709. [PubMed: 16799460]
19. Giacobini P, Messina A, Morello F, et al. Semaphorin 4D regulates gonadotropin hormone-releasing hormone-1 neuronal migration through PlexinB1-Met complex. J Cell Biol. 2008;183(3):555–566. [PubMed: 18981235]
20. Messina A, Giacobini P. Semaphorin signaling in the development and function of the gonadotropin hormone-releasing hormone system. Front Endocrinol (Lausanne). 2013;4:133. [PubMed: 24065959]
21. Janssen BJ, Robinson RA, Pérez-Brangulí F, et al. Structural basis of semaphorin-plexin signalling. Nature. 2010;467(7319):1118–1122. [PubMed: 20877282]
22. Tong Y, Hota PK, Penachioni JY, et al. Structure and function of the intracellular region of the plexin-b1 transmembrane receptor. J Biol Chem. 2009;284(51):35962–35972. [PubMed: 19843518]
23. Perrot V, Vazquez-Prado J, Gutkind JS. Plexin B regulates Rho through the guanine nucleotide exchange factors leukemia-associated Rho GEF (LARG) and PDZ-RhoGEF. J Biol Chem. 2002;277(45):43115–43120. [PubMed: 12183458]
24. Swiercz JM, Worzfeld T, Offermanns S. ErbB-2 and met reciprocally regulate cellular signaling via plexin-B1. J Biol Chem. 2008; 283(4):1893–1901. [PubMed: 18025083]
25. Marcos S, Monnier C, Rovira X, et al. Defective signaling through plexin-A1 compromises the development of the peripheral olfactory system and neuroendocrine reproductive axis in mice. Hum Mol Genet. 2017;26(11):2006–2017. [PubMed: 28334861]
26. Oleari R, Lettieri A, Paganoni A, Zanieri L, Cariboni A. Semaphorin signaling in GnRH neurons: from development to disease. Neuroendocrinology. 2019;109(3):193–199. [PubMed: 30504719]
27. Kotan LD, Isik E, Turan I, et al. Prevalence and associated phenotypes of PLXNA1 variants in normosmic and anosmic idiopathic hypogonadotropic hypogonadism. Clin Genet. 2019;95(2):320–324. [PubMed: 30467832]
28. Yang H, Wang K. Genomic variant annotation and prioritization with ANNOVAR and wANNOVAR. Nat Protoc. 2015;10(10):1556–1566. [PubMed: 26379229]
29. Yang J, Zhang Y. I-TASSER server: new development for protein structure and function predictions. Nucleic Acids Res. 2015;43(W1) :W174–W181. [PubMed: 25883148]
30. Zhang C, Freddolino PL, Zhang Y. COFACTOR: improved protein function prediction by combining structure, sequence and protein-protein interaction information. Nucleic Acids Res. 2017;45(W1):W291–W299. [PubMed: 28472402]
31. Williams CJ, Headd JJ, Moriarty NW, et al. MolProbity: more and better reference data for improved all-atom structure validation. Protein Sci. 2018;27(1):293–315. [PubMed: 29067766]
32. Zhang Y, Skolnick J. Scoring function for automated assessment of protein structure template quality. Proteins. 2004;57(4):702–710. [PubMed: 15476259]

33. Krieger E, Joo K, Lee J, et al. Improving physical realism, stereochemistry, and side-chain accuracy in homology modeling: four approaches that performed well in CASP8. Proteins. 2009;77(Suppl 9):114–122. [PubMed: 19768677]
34. Berjanskii M, Zhou J, Liang Y, Lin G, Wishart DS. Resolution-by-proxy: a simple measure for assessing and comparing the overall quality of NMR protein structures. J Biomol NMR. 2012;53(3):167–180. [PubMed: 22678091]
35. Pahari S, Li G, Murthy AK, et al. SAAMBE-3D: predicting effect of mutations on protein-protein interactions. Int J Mol Sci. 2020;21(7):2563. [PubMed: 32272725]
36. Rodrigues CHM, Myung Y, Pires DEV, Ascher DB. mCSM-PPI2: predicting the effects of mutations on protein-protein interactions. Nucleic Acids Res. 2019;47(W1):W338–W344. [PubMed: 31114883]
37. Zhang N, Chen Y, Lu H, et al. MutaBind2: predicting the impacts of single and multiple mutations on protein-protein interactions. iScience. 2020;23(3):100939. [PubMed: 32169820]
38. Chen Y, Lu H, Zhang N, Zhu Z, Wang S, Li M. PremPS: predicting the impact of missense mutations on protein stability. PLoS Comput Biol. 2020;16(12):e1008543. [PubMed: 33378330]
39. Rodrigues CH, Pires DE, Ascher DB. DynaMut: predicting the impact of mutations on protein conformation, flexibility and stability. Nucleic Acids Res. 2018;46(W1):W350–W355. [PubMed: 29718330]
40. Radovick S, Wray S, Lee E, et al. Migratory arrest of gonadotropin-releasing hormone neurons in transgenic mice. Proc Natl Acad Sci USA. 1991;88(8):3402–3406. [PubMed: 2014260]
41. Larco DO, Semsarzadeh NN, Cho-Clark M, Mani SK, Wu TJ. β-Arrestin 2 is a mediator of GnRH-(1–5) signaling in immortalized GnRH neurons. Endocrinology. 2013;154(12):4726–4736. [PubMed: 24140715]
42. Giacobini P, Messina A, Wray S, et al. Hepatocyte growth factor acts as a motogen and guidance signal for gonadotropin hormone-releasing hormone-1 neuronal migration. J Neurosci. 2007;27(2):431–445. [PubMed: 17215404]
43. Scott EM, Halees A, Itan Y, et al. Characterization of Greater Middle Eastern genetic variation for enhanced disease gene discovery. Nat Genet. 2016;48(9):1071–1076. [PubMed: 27428751]
44. Richards S, Aziz N, Bale S, et al. Standards and guidelines for the interpretation of sequence variants: a joint consensus recommendation of the American College of Medical Genetics and Genomics and the Association for Molecular Pathology. Genet Med. 2015;17(5):405–424. [PubMed: 25741868]
45. Saengkaew T, Ruiz-Babot G, David A, et al. Whole exome sequencing identifies deleterious rare variants in CCDC141 in familial selflimited delayed puberty. NPJ Genom Med. 2021;6(1):107. [PubMed: 34930920]
46. Sykiotis GP, Plummer L, Hughes VA, et al. Oligogenic basis of isolated gonadotropin-releasing hormone deficiency. Proc Natl Acad Sci USA. 2010;107(34):15140–15144. [PubMed: 20696889]
47. Gianetti E, Tusset C, Noel SD, et al. TAC3/TACR3 mutations reveal preferential activation of gonadotropin-releasing hormone release by neurokinin B in neonatal life followed by reversal in adulthood. J Clin Endocrinol Metab. 2010;95(6):2857–2867. [PubMed: 20332248]
48. Bouilly J, Messina A, Papadakis G, et al. DCC/NTN1 complex mutations in patients with congenital hypogonadotropic hypogonadism impair GnRH neuron development. Hum Mol Genet. 2018;27(2):359–372. [PubMed: 29202173]
49. Xu C, Messina A, Somm E, et al. KLB, encoding beta-Klotho, is mutated in patients with congenital hypogonadotropic hypogonadism. EMBO Mol Med. 2017;9(10):1379–1397. [PubMed: 28754744]
50. Sidhoum VF, Chan YM, Lippincott MF, et al. Reversal and relapse of hypogonadotropic hypogonadism: resilience and fragility of the reproductive neuroendocrine system. J Clin Endocrinol Metab. 2014;99(3):861–870. [PubMed: 24423288]
51. Giacobini P, Giampietro C, Fioretto M, et al. Hepatocyte growth factor/scatter factor facilitates migration of GN-11 immortalized LHRH neurons. Endocrinology. 2002;143(9):3306–3315. [PubMed: 12193542]
52. Tran TS, Kolodkin AL, Bharadwaj R. Semaphorin regulation of cellular morphology. Annu Rev Cell Dev Biol. 2007;23:263–292. [PubMed: 17539753]

53. Kotan LD, Ternier G, Cakir AD, et al. Loss-of-function variants in SEMA3F and PLXNA3 encoding semaphorin-3F and its receptor plexin-A3 respectively cause idiopathic hypogonadotropic hypogonadism. Genet Med. 2021;23(6):1008–1016. [PubMed: 33495532]
54. Miraoui H, Dwyer AA, Sykiotis GP, et al. Mutations in FGF17, IL17RD, DUSP6, SPRY4, and FLRT3 are identified in individuals with congenital hypogonadotropic hypogonadism. Am J Hum Genet. 2013;92(5):725–743. [PubMed: 23643382]
55. Balasubramanian R, Crowley WF Jr. Reproductive endocrine phenotypes relating to CHD7 mutations in humans. Am J Med Genet C Semin Med Genet. 2017;175(4):507–515. [PubMed: 29152903]
56. Hanchate NK, Giacobini P, Lhuillier P, et al. SEMA3A, a gene involved in axonal pathfinding, is mutated in patients with Kallmann syndrome. PLoS Genet. 2012;8(8):e1002896. [PubMed: 22927827]
57. Känsäkoski J, Fagerholm R, Laitinen EM, et al. Mutation screening of SEMA3A and SEMA7A in patients with congenital hypogonadotropic hypogonadism. Pediatr Res. 2014;75(5):641–644. [PubMed: 24522099]
58. Young J, Metay C, Bouligand J, et al. SEMA3A deletion in a family with Kallmann syndrome validates the role of semaphorin 3A in human puberty and olfactory system development. Hum Reprod. 2012;27(5):1460–1465. [PubMed: 22416012]
59. Cariboni A, André V, Chauvet S, et al. Dysfunctional SEMA3E signaling underlies gonadotropin-releasing hormone neuron deficiency in Kallmann syndrome. J Clin Invest. 2015;125(6):2413–2428. [PubMed: 25985275]
60. Oleari R, Andrè V, Lettieri A, et al. A novel SEMA3G mutation in two siblings affected by syndromic GnRH deficiency. Neuroendocrinology. 2021;111(5):421–441. [PubMed: 32365351]
61. Zhou C, Niu Y, Xu H, et al. Mutation profiles and clinical characteristics of Chinese males with isolated hypogonadotropic hypogonadism. Fertil Steril. 2018;110(3):486–495. e485. [PubMed: 30098700]
62. Chen Y, Sun T, Niu Y, et al. A partial loss-of-function variant in GNRNR gene in a Chinese cohort with idiopathic hypogonadotropic hypogonadism. Transl Androl Urol. 2021;10(4):1676–1687. [PubMed: 33968656]
63. Chen Y, Sun T, Niu Y, et al. Correlations among genotype and outcome in chinese male patients with congenital hypogonadotropic hypogonadism under HCG treatment. J Sex Med. 2020;17(4):645–657. [PubMed: 32171629]
64. Deng S, Hirschberg A, Worzfeld T, et al. Plexin-B2, but not Plexin-B1, critically modulates neuronal migration and patterning of the developing nervous system in vivo. J Neurosci. 2007;27(23):6333–6347. [PubMed: 17554007]
65. Giraudon P, Vincent P, Vuaillat C, et al. Semaphorin CD100 from activated T lymphocytes induces process extension collapse in oligodendrocytes and death of immature neural cells. J Immunol. 2004;172(2):1246–1255. [PubMed: 14707103]
66. Lontos K, Adamik J, Tsagianni A, Galson DL, Chirgwin JM, Suvannasankha A. The role of semaphorin 4D in bone remodeling and cancer metastasis. Front Endocrinol (Lausanne). 2018;9:322. [PubMed: 29971044]
67. Kong Y, Janssen BJ, Malinauskas T, et al. Structural basis for plexin activation and regulation. Neuron. 2016;91(3):548–560. [PubMed: 27397516]

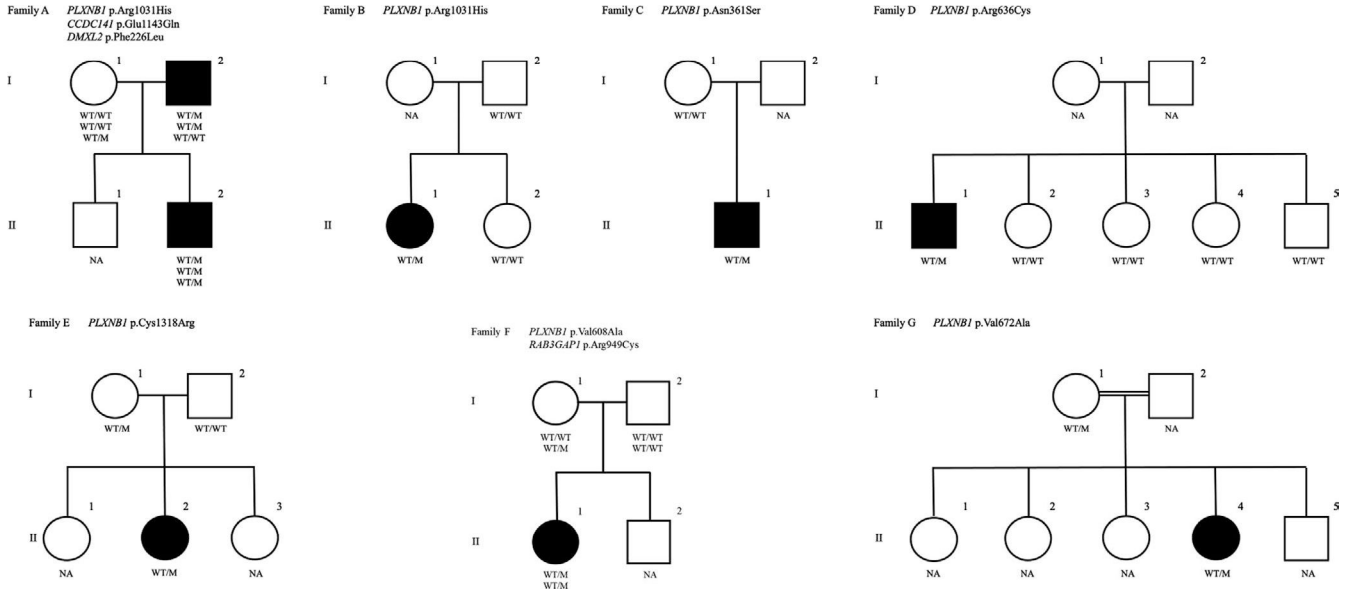

FIGURE 1.

Pedigrees of the families with PLXNB1 and other gene variants are shown. Affected males and females are represented by black squares and black circles, respectively. White square symbols indicate unaffected male family members, white circle symbols represent unaffected female family members, and the double line indicates consanguinity. Under each symbol are the genotypes in the same order as the gene and variant descriptions, with WT and M denoting wild-type and mutant, respectively. NA denotes that no DNA specimen is available from this individual

(A)

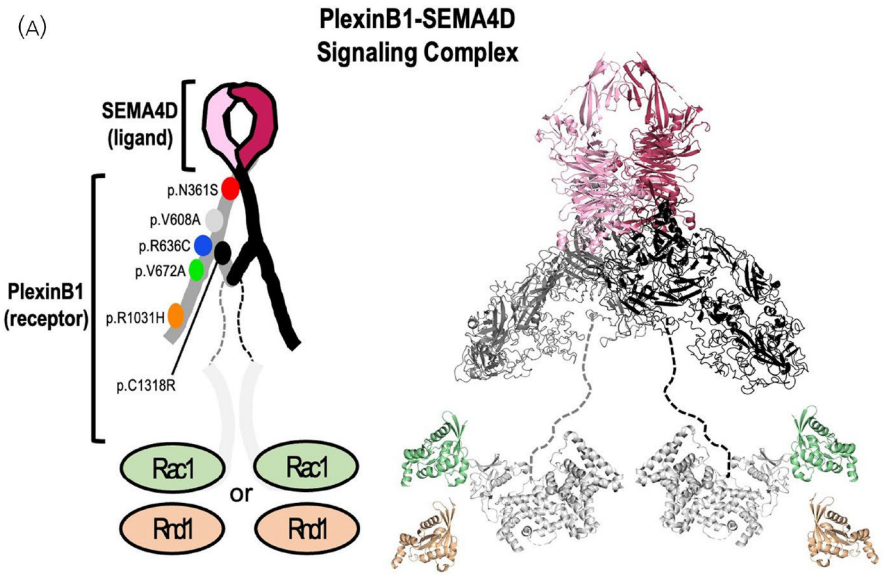

(B)

PlexinB1 variants found in IHH families.

Amino Acid change	cDNA change	Domain Location	Summary
p.Asn361Ser	c.A1082G	SEMA	Destabilize folding (1 of 2), Stabilize folding (1 of 2) Decrease affinity (3 of 3)
p.Val608Ala	c.1823T>C	IPT1	Destabilize folding (2 of 2) Decrease affinity (3 of 3)
p.Arg636Cys	c.1906C>T	PSI2	Destabilize folding (1 of 2), Stabilize folding (1 of 2) Decrease affinity (3 of 3)
p.Val672Ala	c.2015T>C	Mucin	Destabilize folding (2 of 2) Decrease affinity (3 of 3)
p.Arg1031His	c.3092G>A	PSI3	Destabilize folding (2 of 2) Decrease affinity (3 of 3)
p.Cys1318Arg	c.3952T>C	IPT5	Destabilize folding (1 of 2), Stabilize folding (1 of 2) Increase affinity (1 of 3), No change affinity (2 of 3)

FIGURE 2.

The location and deleterious properties of six novel idiopathic hypogonadotropic hypogonadism (IHH) variants in PLXNB1. (A) Left: cartoon illustration showing the interaction between dimeric Sema4D (ligand) and dimeric PlexinB1 (receptor) with IHH mutations labeled. Right: YASARA energy-minimized signaling complex showing the interaction between dimeric Sema4D (ligand, pink and red), dimeric PlexinB1 (receptor, gray and black), and Rho GTPases (green = Rac1, gold = Rnd1) derived from predictive modeling and crystals (Protein Data Bank: 3OL2, 3HM6, 3SUA and 2REX). (B) Six *PLXNB1* variations (p. N361S, p.V608A, p.R636C, p.V672A, p.R1031H, and p.C1318R, shown on the left) were examined using in silico mutagenesis. p.V608A, pV672A, and p.R1031H were predicted to be deleterious to the interaction of PlexinB1 with its binding partners and its protein folding

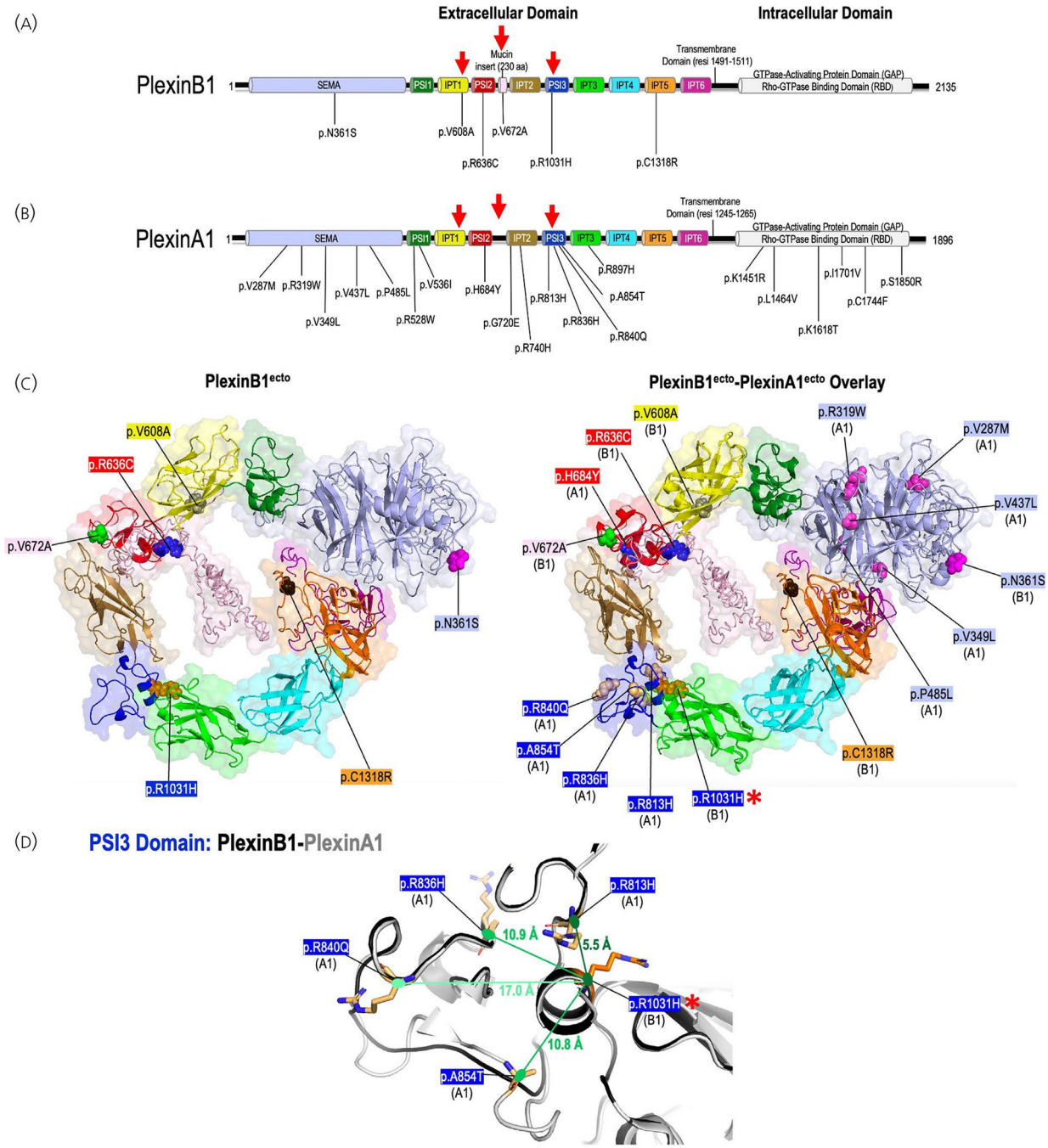

FIGURE 3.

Alignment of Kallmann syndrome (KS)/idiopathic hypogonadotropic hypogonadism (IHH) mutations found in PlexinB1 and PlexinA1. (A) Linear depiction of PlexinB1 protein domains based on prior reports[21,67] with mutations identified in the present study shown. (B) Linear depiction of PlexinA1 protein domains (adapted from[67] and[25] with mutations identified in Marcos et al.[25] and Kotan et al.[27] Red arrows in (A) and (B) highlight domains housing variants predicted to be deleterious to PlexinB1 function (Figure 1B). (C) Left: Full-length PlexinB1^{ecto} predicted by I-TASSER indicating the location of the

six IHH mutations in PlexinB1 (p.N361S, p.V608A, p.R636C, p.V672A, p.R1031H, and p.C1318R, colors of variants correspond to domains in A and B). Right: Overlay of PlexinB1$^{ecto(I-TASSER)}$ and PlexinA1 crystal (Protein Data Bank: 5L56) with mutations indicated by subdomain/location. (D) High magnification of the substitutions found in the PSI3 domain of PlexinB1 (p.R1031H, asterisk) and Plexin A1 (p.R813H, p.R836H, p.R840Q, p.A854T). The PlexinB1 and two of the four PlexinA1 variants are an arginine to histidine substitution. Angstrom measurements, ranging from 5.5A–17.0 A (green lines) are shown for PlexinA1 mutants compared to p.R1031H (PlexinB1, asterisk)

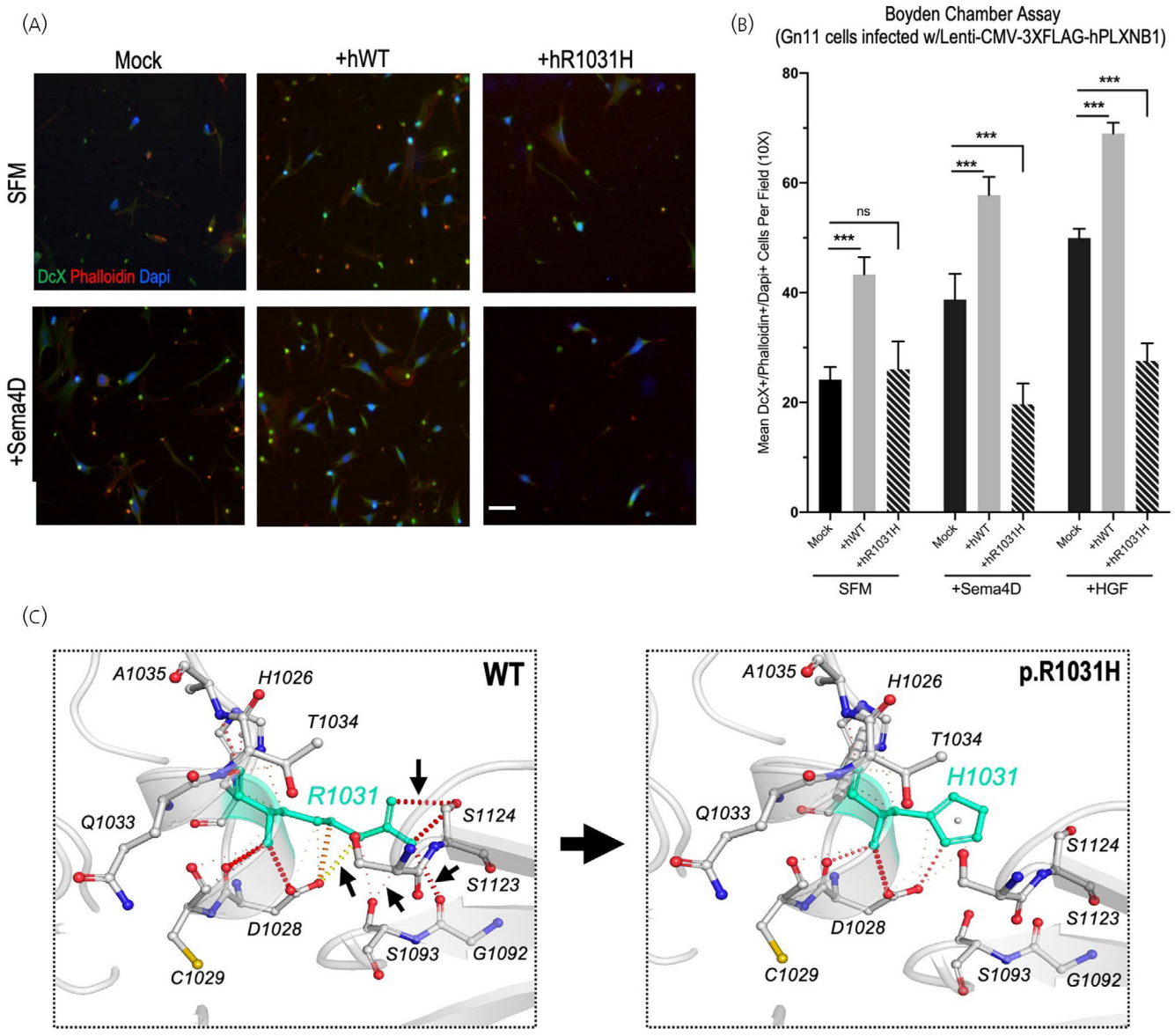

FIGURE 4.

p.R1031H affects PlexinB1 function and structure. (A, B) Boyden chamber assays using Lenti-CMV-hPLXNB1 (+hWT) infected Gn11 cells showed +hWT increased the basal level of migration (SFM, $p = .0009$) and response to PLXBN1 agonists (Sema4D, $p = .0010$; hepatocyte growth factor [HGF], $p = .0010$) compared to mock infected Gn11 cells (Lent-CMV-GFP). By contrast, +hR1031H impaired cell migration in response to agonists (Sema4D, $p = .0009$; HGF, $p = .0002$), but did not significantly alter basal migration compared to mock infected SFM (indicated by NS). (C) High magnification images of DynaMut prediction of the intrachain bonds in wild-type (WT) (left) compared to p.R1031H mutant protein (right) showing loss of intrachain bonds (black arrows, WT) in mutant. One-way ANOVA followed by Fisher's post-hoc least significant difference was used for analysis of results in B (***$p < .001$). Scale bar = 50 um in (A)

TABLE 1

Clinical and laboratory characteristics of individuals with PLXNB1 mutations at initial presentations and after prolonged follow-up periods

Family/ individual number	Variant	Age at diagnosis (years)	Age at last visit (years)	Sex	Initial basal LH (mIU mL^{-1})/ estradiol (ng dL^{-1}) or testosterone (ng dL^{-1})	Initial stimulated maximum LH (mIU mL^{-1})	Last basal LH (mIU mL^{-1})/ estradiol (ng dL^{-1}) or testosterone (ng dL^{-1})	Olfaction	Signs of congenital hypogonadism	Initial complaint at presentation	Final reproductive diagnosis after follow-up
A I–1	p. Arg1031His	17	46	M	NA	NA		Normosmic	None	Pubertal delay	Constitutional delay in growth and puberty
A II-2	p. Arg1031His	14.2	20	M	0.40/12.0	1.67	3.29/443	Normosmic	None	Pubertal delay	Constitutional delay in growth and puberty
B II-1	p. Arg1031His	15.2	20	F	0.18/< 20	2.45	0.15/1.85	Normosmic	None	Pubertal delay, Primary amenorrhea	IHH
C II-1	p. Asn361Ser	21	28	M	2.28/193	8.46	NA	Normosmic	Cryptorchidism	Pubertal delay	IHH, clinically partially recovered
D II-1	p. Arg636Cys	22	30	M	0.32/10	NA	0.26/73	Normosmic	None	Pubertal delay	IHH
E II–2	p. Cys1318Arg	15.7	21	F	0.21/0.8	1.15	0.20/0.2	Normosmic	None	Pubertal delay, Primary amenorrhea	IHH
F II-1	p. Val608Ala	17	24	F	0.10/0.5	4.10	< 0.3/2.9	Normosmic	None	Pubertal delay, Primary amenorrhea	IHH
G II–4	p. Val672Ala	15.6	27	F	0.5/0.5	2.9	0.9/0.1	Normosmic	None	Pubertal delay, Primary amenorrhea	IHH

Abbreviations: M, male; F, female; LH, luteinizing hormone; NA, not available.

TABLE 2

The molecular genetic characteristics of the heterozygous PLXNB1 variants

Family/individual no.	Variant at cDNA level	Variant at protein level	CADD score	GME	gnomAD	ACMG/AMP evaluation	Additional gene mutations
A I-1	c.3092G>A	p. Arg1031His	21.8	Absent	0.0002	VUS: PM1	*CCDC141* p. Glu1143Gln
A II-2	c.3092G>A	p. Arg1031His	21.8	Absent	0.0002	VUS: PM1	*CCDC141* p. Glu1143Gln and *DMXL2* p. Phe226Leu
B II-1	c.3092G>A	p. Arg1031His	21.8	Absent	0.0002	VUS: PM1	
C II-1	c.1082 A>G	p. Asn361Ser	15.1	Absent	0.000007	VUS: PM1, PM2, BP4	
D II-1	c.1906C>T	p. Arg636Cys	20.4	Absent	0.00001	VUS: PM1, PM2	
E II-2	c.3952T>C	p. Cys1318Arg	22.2	Absent	0.00001	VUS: PM1, PM2	
F II-1	c.1823T>C	p. Val608Ala	22.4	Absent	Absent	VUS: PM1, PM2	*RAB3GAP1* p. Arg949Cys
G II-4	c.2015T>C	p. Val672Ala	22.6	Absent	Absent	VUS: PM1, PM2	

Abbreviations: BP, benign supporting; CADD, Combined Annotation Dependent Depletion (https://cadd.gs.washington.edu). Variants are described according to the RefSeq numbers following the gene names: PLXNB1, NM_001130082; CCDC141, NM_173648; DMXL2, NM_001174116; GME, The Greater Middle East Variome Project; gnomAD, The Genome Aggregation Consortium; PM, pathogenic moderate; RAB3GAP1, NM_001172435. All variants are heterozygous; VUS, variant uncertain significance.